

Easy, operable ionic polymer metal composite actuator based on a platinum-coated sulfonated poly(vinyl alcohol)-polyaniline composite membrane

Ajhar Khan,¹ Inamuddin,¹ Ravi Kant Jain²

¹Department of Applied Chemistry, Faculty of Engineering and Technology, Aligarh Muslim University, Aligarh 202002, India

²Design of Mechanical System (DMS)/Micro Robotics Laboratory, Central Mechanical Engineering Research Institute, Council of Scientific and Industrial Research, Durgapur 713209, West Bengal, India

Correspondence to: Inamuddin (E-mail: inamuddin@rediffmail.com)

ABSTRACT: In this study, an electric-stimulus-responsive bending actuator based on a platinum (Pt)-coated sulfonated poly(vinyl alcohol) (SPVA)-polyaniline (PANI) composite membrane was developed. The SPVA-PANI membrane was prepared by a solution casting method; it showed good electrochemical properties and an adequate ion-exchange capacity of 1.6 mequiv/g of dry membrane. The water uptake by the membrane with 4 h of immersion time at 45 °C was found to be 425%. The SPVA-PANI composite membrane based ionic polymer metal composite (IPMC) actuator prepared by the coating of Pt metal layers on both sides of the membrane by an electroless plating process showed a good proton conductivity of 1.75×10^{-3} S/cm. The smooth and uniform coating of Pt on both surfaces of the membrane, as indicated by scanning electron micrographs, seemed to be responsible for the slow water loss that is necessary for the long life of an IPMC actuator. The maximum water loss was 48% at 6 V for 12 min. This indicated the better performance of the IPMC membrane when an electric potential was applied. According to electromechanical characterization, the maximum tip displacement was 14.5 mm at 5.25 V. A multifinger IPMC membrane based microgripping system was developed, and it showed potential for microrobotics application. © 2016 Wiley Periodicals, Inc. *J. Appl. Polym. Sci.* **2016**, *133*, 43787.

KEYWORDS: composites; films; membranes

Received 16 February 2016; accepted 15 April 2016

DOI: 10.1002/app.43787

INTRODUCTION

Ionic polymer metal composites (IPMCs) belong to one of the most promising groups of electroactive polymeric actuators because of their large and fast bending deformation, which is produced by a fairly low external electrical stimulus of 1–6 V.^{1–6} IPMC actuators have received a great deal of attention from researchers and industry engineers because of their many potential applications, such as in dynamic sensors, artificial muscles, and robotic actuators.^{7–12} IPMCs are typically composed of an ion-conductive layer of polymeric material sandwiched between platinum (Pt) or gold electrode layers; this material bends toward the cathode because of the directional transport of mobile cations along with the water molecules in the interior part of the IPMC membrane under an applied electric potential.^{13,14} The commercially available perfluorinated polymer Nafion membrane developed by the well-renowned company DuPont has excellent mechanical and chemical properties and a high proton conductivity.^{15–19} However, perfluorinated IPMC actuators show good electromechanical performances, but there

are some limitations, including a low blocking force, back relaxation, high cost, and environmental unfriendliness. Therefore, to replace perfluorinated polymers and improve the performance of IPMC actuators, nonperfluorinated electroactive polymers are considered to be important alternatives.²⁰ Interestingly, various types of nonperfluorinated polymers, such as sodium sulfonate-functionalized poly(ether ether ketone),²¹ sulfonated poly(styrene-*b*-ethylene-*co*-butylene-*b*-styrene),²² sulfonated poly(arylenethioether sulfone)s,²³ sulfonated poly(styrene-*ran*-ethylene),²⁴ kraton polymer,²⁵ sulfonated poly(vinyl alcohol) (SPVA)/polypyrrole,²⁶ polyacrylonitrile-kraton-graphene,²⁷ and poly(3,4-ethylene dioxathiophene)/polystyrene sulfonate zirconium(IV) phosphate,²⁸ have been used in the recent past for the development of IPMC actuators.^{29–31} However, the IPMC actuators prepared with sulfonated nonperfluorinated ionic polymers have been found to show very slow response times and back relaxation.^{32–34} To improve the properties of actuators, it was considered worthwhile to develop an SPVA-polyaniline (PANI) polymer membrane based IPMC. The conducting nature and redox cyclability of PANI improve the bending rate

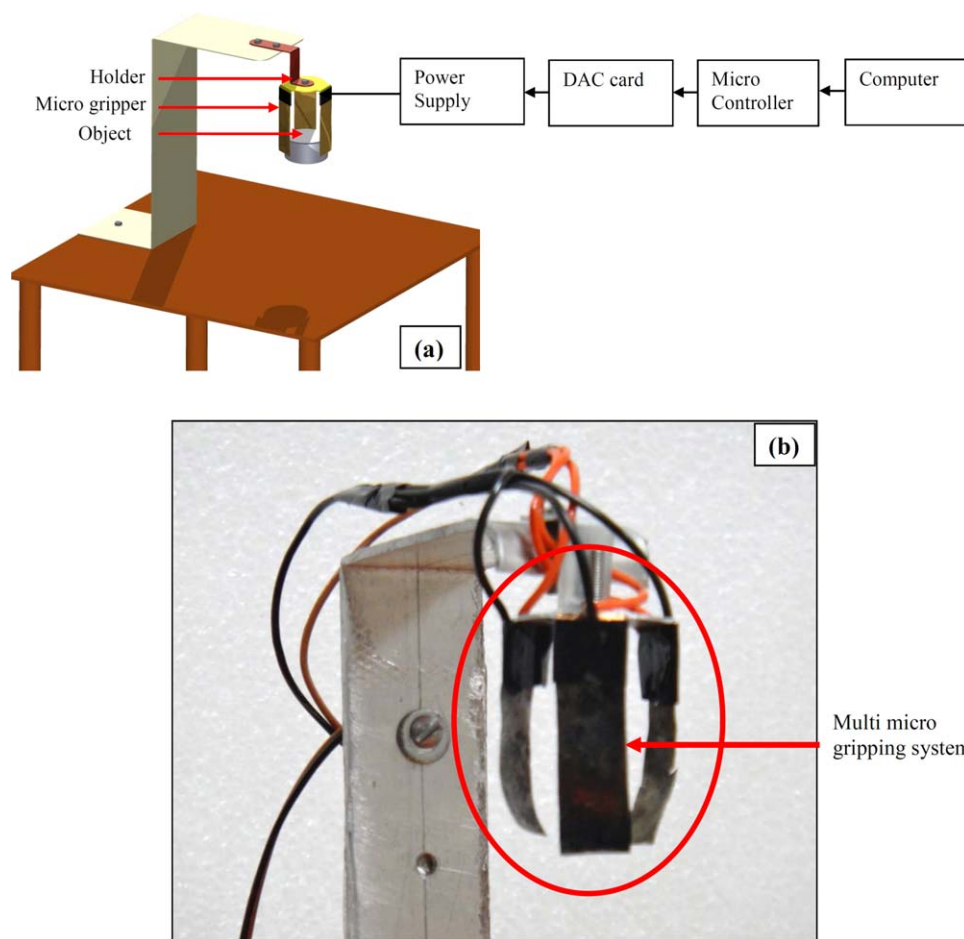


Figure 1. (a) Computer-aided design model of multifinger-based microgripping and (b) detailed view of the IPMC-based microgripper. [Color figure can be viewed in the online issue, which is available at wileyonlinelibrary.com.]

and displacement and minimize the back-relaxation phenomenon. Thus, an SPVA–PANI–Pt based IPMC actuator can provide an easy and reliable solution for the realization of novel actuators and the possibility of their industrial applications. The major interesting features of this research include the following:

1. The design and development of novel SPVA–PANI IPMC membranes with a Pt electrode (SPVA–PANI–Pt) based microgripping system.
2. Characterization of an SPVA–PANI–Pt ionic actuator and the demonstration of a microgripping system.

Both of these contributions will lead to a new era of IPMC actuators with an SPVA–PANI–Pt, which has a large deflection capability for the development of the microrobotic system. The proposed IPMC has tremendous potential with its large flexible behavior compared to other smart materials, such as piezoelectric, shape-memory alloy, and electroactive polymers. Other important advantages of this study include the small operating voltage (0–5.25 V), light weight, use in different sizes and shapes, and need for an uncomplicated controller to develop the micro-robots. From the analysis of the bending behavior of the SPVA–PANI–Pt IPMC membrane actuator with voltage, the schematic diagram of the experimental setup is shown in Figure 1.

EXPERIMENTAL

Materials Used for the Development of an SPVA–PANI–Pt Based IPMC Actuator

Poly(vinyl alcohol) (PVA; cold; Central Drug House Pvt., Ltd., India), 4-sulfophthalic acid (50 wt % solution in water, Sigma-Aldrich Chemie Pvt., Ltd.), aniline ($C_6H_5NH_2$; Thermo Fisher Scientific Pvt., Ltd., India), potassium peroxodisulfate ($K_2S_2O_8$; extrapure), and ammonium hydroxide (NH_4OH ; 25%; Merck Specialties Pvt., Ltd., India), tetra-amineplatinum(II) chloride monohydrate [$Pt(NH_3)_4Cl_2 \cdot H_2O$ (crystalline); Alfa Aesar], and sodium borohydride ($NaBH_4$; Thomas Baker Pvt., Ltd., India) were used as received without further purification.

Preparation of the Reagent Solutions

Solutions of 10% v/v $C_6H_5NH_2$ and 0.1 M $K_2S_2O_8$ were prepared in 1 M HCl. Aqueous solutions of $Pt(NH_3)_4Cl_2 \cdot H_2O$ (0.04 M), NH_4OH (5.0%), and $NaBH_4$ (5.0%) were prepared in demineralized water.

Fabrication of the Membrane

An aqueous solution of PVA was prepared by the dissolution of 4 g of PVA in 100 mL of demineralized water at 60 °C for 6 h with constant stirring. The solution was filtered, and to the filtrate, 4 mL of 4-sulfophthalic acid was added for sulfonation; this was followed by continuous stirring for 15 h at 60 °C. The

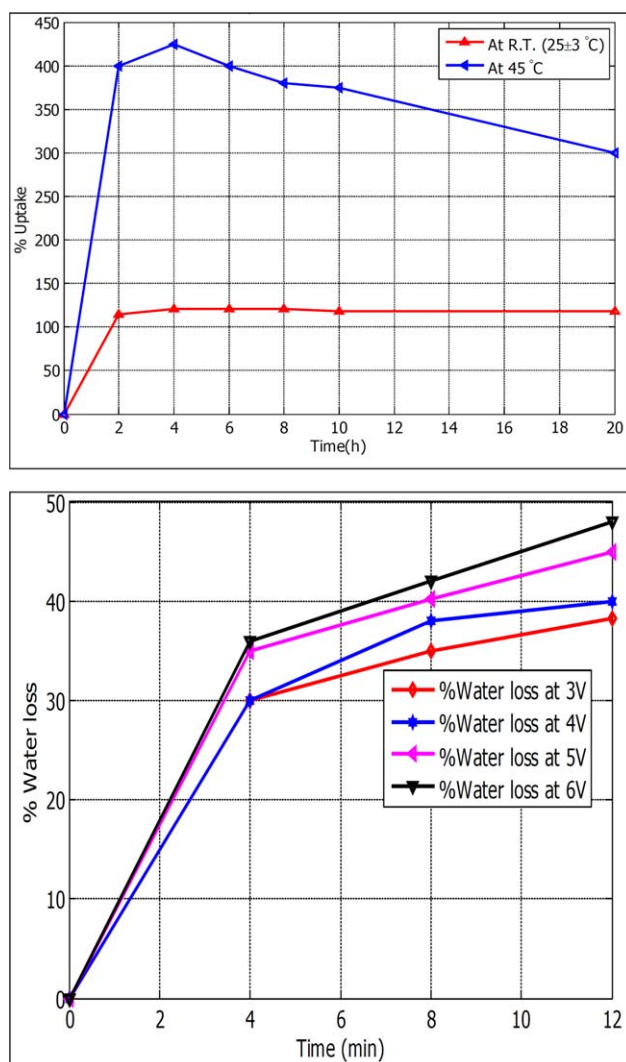


Figure 2. (a) Percentage water uptake of the SPVA-PANI membrane and (b) percentage water loss of the SPVA-PANI membrane. R.T. = room temperature. [Color figure can be viewed in the online issue, which is available at wileyonlinelibrary.com.]

homogeneous solution of the SPVA polymer was then cast into a Petri dish ($50 \times 17 \text{ mm}^2$) covered with Whatman filter paper (No. 1) for the slow evaporation of the solvent at 45 °C in a thermostat oven. After drying, the membrane was removed from the Petri dish with the help of forceps and a spatula. We crosslinked the membrane by placing it in a thermostated oven at 150 °C for up to 1 h. The *in situ* polymerization of $\text{C}_6\text{H}_5\text{NH}_2$ on the SPVA membrane was carried out by the placement of the dry membrane in 50 mL of $\text{C}_6\text{H}_5\text{NH}_2$ solution in a conical flask and the subsequently addition of 60 mL of $\text{K}_2\text{S}_2\text{O}_8$ solution. This was followed by constant stirring for 0.5 h at a temperature not exceeding 10 °C. The conical flask was covered with aluminum foil and kept in a refrigerator for 24 h for digestion.

Ion-Exchange Capacity, Proton Conductivity, and Water Uptake

The ion-exchange capacity, proton conductivity, and water-uptake capacity of the SPVA-PANI membrane were measured, as reported by Inamuddin *et al.*²⁰

Chemical Plating

An electroless plating method was used to coat the Pt metal on the surface of the SPVA-PANI membrane.^{35,36} The SPVA-PANI membrane surfaces were roughened from both sides with mild sandpaper; this was followed by cleaning with an ultrasonicator for 20 min. The membranes were immersed in 2 M HCl for 6 h at room temperature ($25 \pm 3 \text{ }^\circ\text{C}$) and neutralized with double-distilled water (DMW). To coat the Pt electrode, the SPVA-PANI membrane was treated with aqueous solutions of $\text{Pt}(\text{NH}_3)_4\text{Cl}_2 \cdot \text{H}_2\text{O}$ (4.5 mL) and NH_4OH (1 mL). The membrane was left in the reaction vessel for 8 h at room temperature for digestion. After the absorption of Pt ions, the membrane was rinsed with DMW to remove excess Pt ions from the surface of the membrane. The reduction of Pt ions into Pt metal was carried out by the addition of an aqueous solution of NaBH_4 (1 mL) five to six times at 20-min intervals. Finally, an aqueous solution of NaBH_4 (5 mL) was added and stirred for 1.5 h. After it was washed with DMW, the membrane was immersed in a 0.1 M HCl solution for the termination of the reduction process. As the material hydrated, the cations diffused toward an electrode on the material surface under an applied electric field. Inside the polymer structure, anions were interconnected as clusters; this provided channels for the cations to flow toward the electrode.¹ This motion of ions caused the structure to bend toward the anode.

Characterization of the Membrane

The Fourier transform infrared spectrum of SPVA-PANI membrane was recorded between 500 and 4000 cm^{-1} with a PerkinElmer spectrometer. The thermal stability of the SPVA-PANI-Pt membrane was determined by a thermogravimetric analysis instrument (Pyris 1-HT thermogravimetric analyzer, PerkinElmer) at a heating rate of $10 \text{ }^\circ\text{C}/\text{min}$ in an N_2 atmosphere. The surface morphology of the SPVA-PANI-Pt membrane before and after actuation was examined with scanning electron microscopy (JSM6510 LV, JEOL, Japan). Water loss from the IPMC membrane was determined at 3, 4, 5, and 6 V for different time intervals (4, 8, and 12 min).

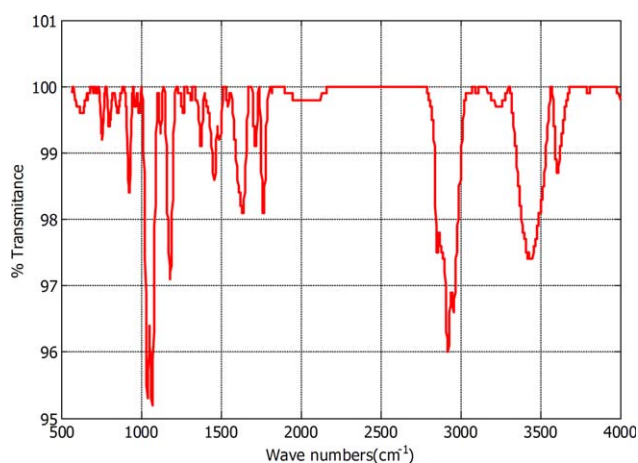


Figure 3. Fourier transform infrared spectrum of the SPVA-PANI-Pt membrane. [Color figure can be viewed in the online issue, which is available at wileyonlinelibrary.com.]

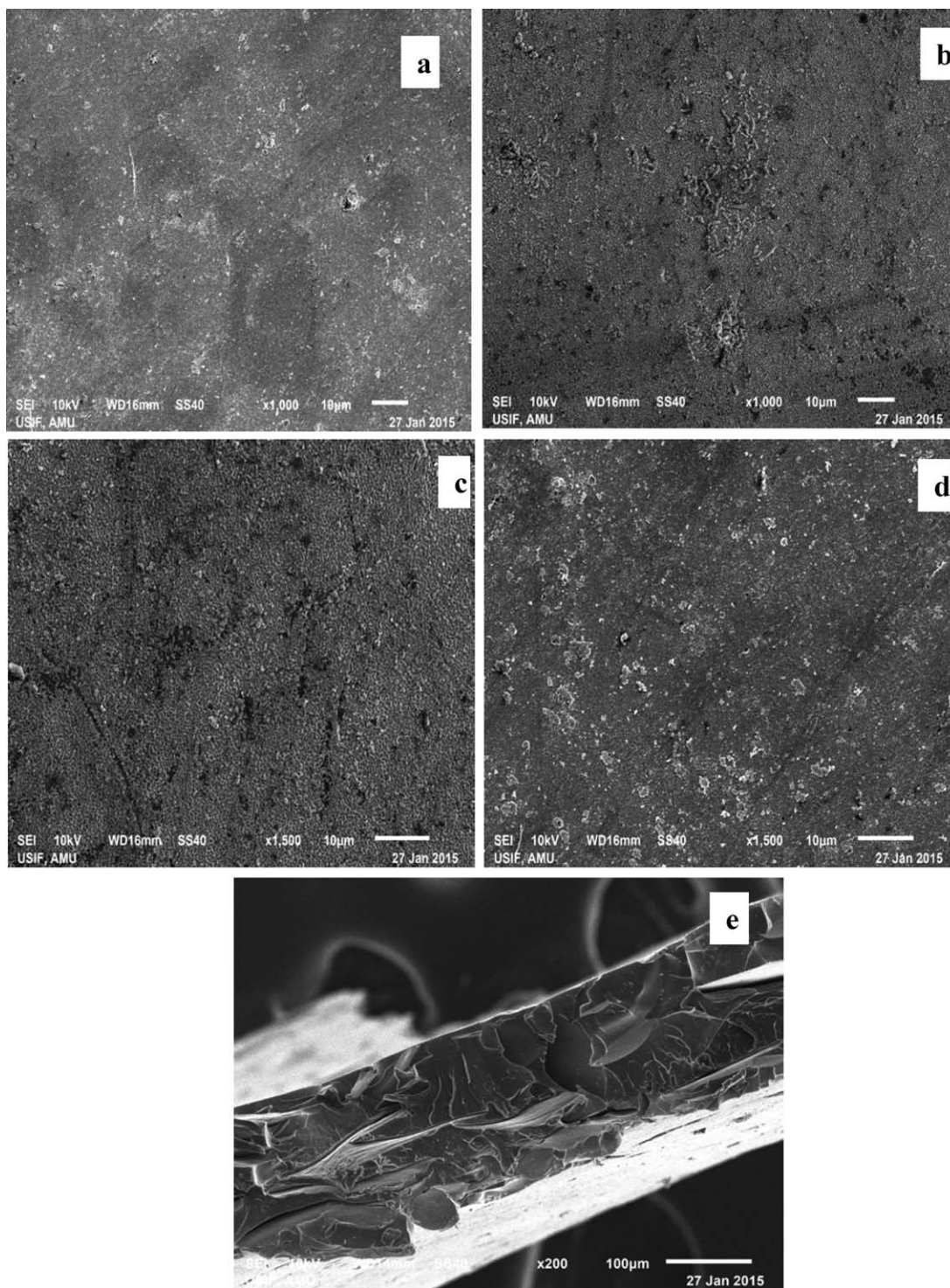


Figure 4. Scanning electron microscopy images of the SPVA–PANI–Pt IPMC membranes at different magnifications: (a,c) before actuation, (b,d) after actuation, and (e) cross-sectional view.

Design of the SPVA–PANI–Pt IPMC Actuator Based Microgripping System

To develop the microgripping system with the SPVA–PANI–Pt actuator, a multifinger-based microgripping system was designed, as shown in Figure 1(a). In the multifinger-based microgripping system, the fingers were constructed with the SPVA–PANI–Pt actuator. This actuator was developed with an

electroless plating method, where SPVA–PANI was the base material. The coating of Pt was done on the surface of SPVA–PANI. All three SPVA–PANI–Pt actuator based fingers were integrated in a wrist. This wrist was clamped with a holder. To activate the SPVA–PANI–Pt actuator based fingers, the voltage [0–5.25 V, direct current (dc)] was applied through a proportional derivative controller. When voltage was supplied through

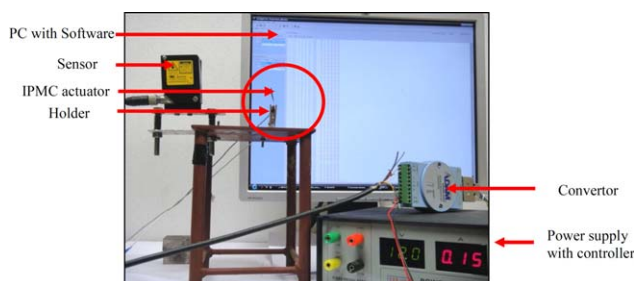


Figure 5. Actual test setup for the bending behavior of the PVA-PANI-Pt ionic actuator. PC = personal computer. [Color figure can be viewed in the online issue, which is available at wileyonlinelibrary.com.]

a controller, all of the fingers bent simultaneously and gripped the object. Afterward, on the release of the voltage, the fingers moved in reverse direction and dropped the object. Detailed dimensions of the IPMC-based microgripper are given in Figure 1(b).

RESULTS AND DISCUSSION

Water uptake was the fundamental parameter for deciding the better performance of the IPMC membrane. The higher the

water uptake was, the better the actuation behavior of the IPMC membrane was.¹⁶ It is evident from Figure 2(a) that the water-uptake capacity of the SPVA-PANI membrane for a duration of 4–8 h at room temperature ($25 \pm 3^\circ\text{C}$) was 120.58%, and after that, saturation occurred. However, there was a significant increase in the water-holding capacity (425%) of the membrane at 45°C with 4 h of immersion. The high water uptake of the ionic polymer membrane supported the increasing hydrophilic nature of the membrane, and this ultimately resulted in its better performance, even at high temperatures and high voltages. The high water-holding capacity of the membrane was advantageous, as more hydrated cations could move through the polymer membrane to actuate the IPMC actuator.¹⁰

The water loss from the membrane was considered a major factor in the short lifetime of the IPMC actuators and the damage of electrode layer. Therefore, the water losses of the wet membranes were determined after the application of electric potentials of 3, 4, 5, and 6 V for different time intervals. After the application of the electric potential, the membrane lost water because of electrolysis; this caused electrode layer damage through the creation of pores on the electrode surface. However, natural evaporation may also

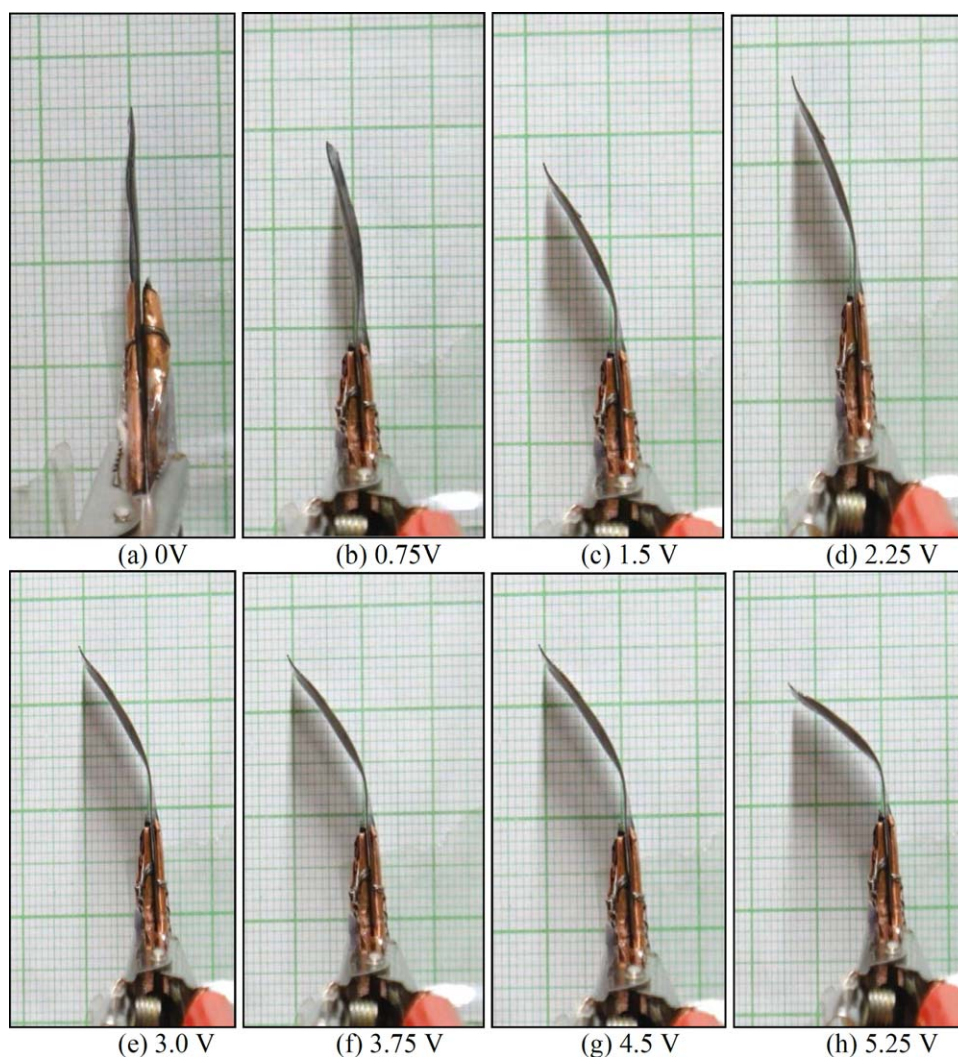


Figure 6. Bending behavior of the IPMC actuator. [Color figure can be viewed in the online issue, which is available at wileyonlinelibrary.com.]

Table I. Experimental Deflection Data with Applied Voltages and Force Data for the SPVA–PANI–Pt Based Ionic Actuator

Voltage (V)	Deflection readings (mm)					Average deflection (mm)	Force readings (gf)					Average force (gf)
	1	2	3	4	5		1	2	3	4	5	
0	0	0	0	0	0	0	0	0	0	0	0	0
0.75	3.1	2.9	3.2	2.8	3.0	3.0	0.009	0.012	0.011	0.008	0.01	0.010
1.50	8.2	8.0	7.8	7.9	8.1	8.0	0.012	0.01	0.009	0.013	0.011	0.011
2.25	9.2	8.8	8.9	9.1	9.0	9.0	0.021	0.019	0.018	0.022	0.02	0.020
3.0	10.2	9.8	9.9	10.1	10.0	10.0	0.031	0.034	0.03	0.032	0.033	0.032
3.75	11.1	10.9	11.2	11.0	10.8	11.0	0.042	0.041	0.04	0.043	0.044	0.042
4.5	12.1	11.9	12.2	11.8	12.0	12.0	0.061	0.059	0.058	0.062	0.06	0.060
5.25	14.5	14.4	14.6	14.7	14.3	14.5	0.08	0.082	0.079	0.081	0.078	0.080
											Mean	0.0364
											Standard deviation	0.0262
											Normal deviation	5.8006

have caused water loss. It is evident from Figure 2(b) that water loss from the IPMC membrane increased with increasing applied voltage from 3 to 6 V for the same period of time. Figure 2(b) also shows the maximum water loss of 48% at 6 V for 12 min of applied voltage. The slower water loss indicated the better performance of the IPMC membrane.

The ion-exchange capacity and proton conductivity of the SPVA–PANI membrane were found to be 1.6 mequiv/g of dry membrane and 1.75×10^{-3} S/cm, respectively. Because of the high ion-exchange capacity of the IPMC membrane, the Pt particles were embedded deeply on the upper and lower surface of the composite membrane through an electroless plating method to create a Pt electrode layer on both sides. The large numbers of Pt nanoparticles and the uniform coating on the upper and lower sides of the IPMC membrane reduced the resistance of the Pt electrode.^{16,35,36} The low resistance was necessary to enable the large tip displacements of the IPMC membrane under an applied low electric potential.^{16,35} The proton conductivity was a key parameter determining the membrane actuation performance; it occurred because of the formation of hydronium ions by the existing protons in the IPMC membrane in the hydrated state. The bending movement of the IPMC membrane was because of the movement of hydrated cations toward the cathode. The high proton conductivity of SPVA–PANI–Pt IPMC was required to increase the electric current of an IPMC and also indicated that more hydrated cations could move quickly toward the cathode side so that the actuator could show a large and fast actuation.¹⁶

The Fourier transform infrared spectrum of the SPVA–PANI membrane is shown in Figure 3. Two broad bands were observed at 3400 and 2946 cm^{-1} ; the former was assigned to the O–H stretching mode in the hydroxyl groups (–OH), and the latter was assigned to the asymmetric –CH₂ stretching band. The bands appearing between 1000 and 1150 cm^{-1} were assigned to C–O stretching.³⁷ The peaks appearing at approximately 1266 and 1750 cm^{-1} were assigned to the asymmetric stretching vibrations of S=O in the sulfonic acid group and the C=O stretching peak of carboxyl acid groups, respectively. The peaks at 1591 cm^{-1} cor-

responded to the C=C stretching vibrations of the quinonoid and benzenoid rings, respectively.³⁸ The peaks at 1300 and 1166 cm^{-1} were attributed to the C–N stretching vibrations of the benzene ring and the stretching of C=N (–N=quinoid=N), respectively. The band at 3410 cm^{-1} was due to the N–H stretching vibrations in the benzene ring.

The surface morphology played an important role in the transport of cations and, therefore, in the bending behavior of the IPMC actuator. Figure 4(a–d) shows the surface micrographs of the SPVA–PANI–Pt membrane before and after the application of electrical voltage. In Figure 4(a,c), smooth and cavity-free surfaces with uniformly coated Pt electrode are clearly shown. The electrode surface of the IPMC membrane after the test of the actuation was damaged to some extent; this resulted in a few negligible cracks, as shown in Figure 4(b,d). Therefore, we assumed that because of the little change in the surface morphology of the IPMC membrane after the application of electrical potential, the water loss from the membrane was due to electrolysis and natural evaporation. The composite polymer membrane sandwiched between Pt electrodes was clear from the cross-sectional scanning electron microscopy micrograph shown in Figure 4(e).

To find the deflection, experiments were conducted with the IPMC actuator made of the SPVA–PANI–Pt material. The IPMC was held in a holder as a cantilever configuration. The voltage between 0 and 5.25 V dc was applied to IPMC through a computer-controlled digital analog card (DAC) and microcontroller. A custom amplifier circuit was developed to provide the desired current rating (50–200 mA) to IPMC. Both surfaces of SPVA–PANI–Pt were connected to this custom amplifier circuit through wires and copper tapes. An electrical signal was provided by a microcontroller. A laser displacement sensor (model OADM 20S4460/S14F, Baumer Electronic, Germany) was used to measure the tip displacement of the IPMC actuator. A converter was used to convert the data from the RS-485 to the RS-232 protocol. The pulse rate was controlled by Docklight V1.8 software through a RS-232 port in a computer. A computer code was written in C programming language where the sampling rate (20 samples/s)

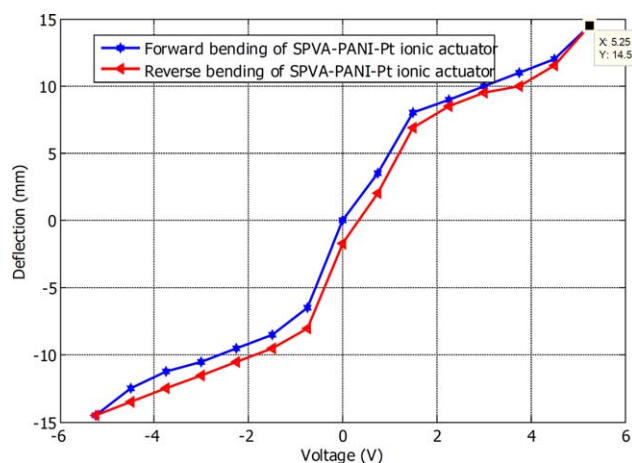


Figure 7. Forward and backward bending behavior of the SPVA-PANI-Pt based ionic actuator. [Color figure can be viewed in the online issue, which is available at wileyonlinelibrary.com.]

was set for controlling the IPMC. The IPMC actuator bent on the positive side at the desired voltage, as shown in Figure 5, and by changing the polarity, the reverse behavior was obtained.

The bending response of IPMC obtained with the SPVA-PANI-Pt material (size = 29 mm length \times 10.5 mm width \times 0.11 mm thickness) at different voltages (0–5.25 V, dc) is shown in Figure 6. The data were collected at different voltages five times (deflections 1–5), as shown in Table I.

To plot the bending characteristics of deflection with voltage, the average of five values at same voltage was taken and plotted (Figure 7). From this figure, it is clear that when the voltage was reduced from high (5.25 V) to low (0 V), the IPMC did not follow the same path to return to its original position. We observed that IPMC had a deflection error of 1.7 mm; this could be minimized through an adjustment of the frequency in the controller. The error bar is plotted in Figure 8.

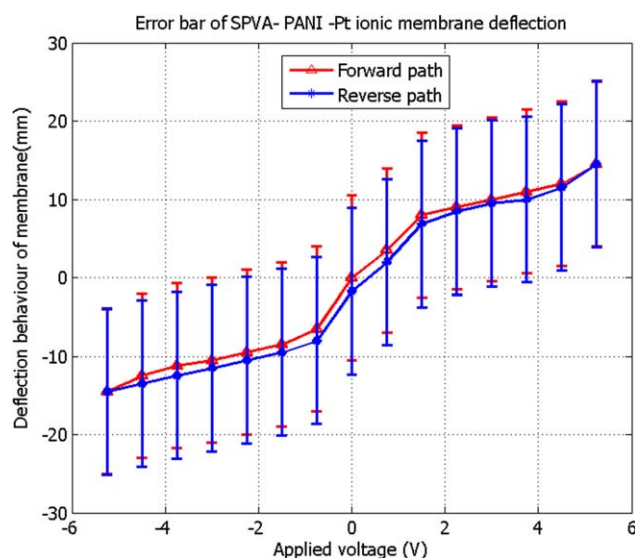


Figure 8. Error bar for the deflection of the SPVA-PANI-Pt ionic membrane. [Color figure can be viewed in the online issue, which is available at wileyonlinelibrary.com.]

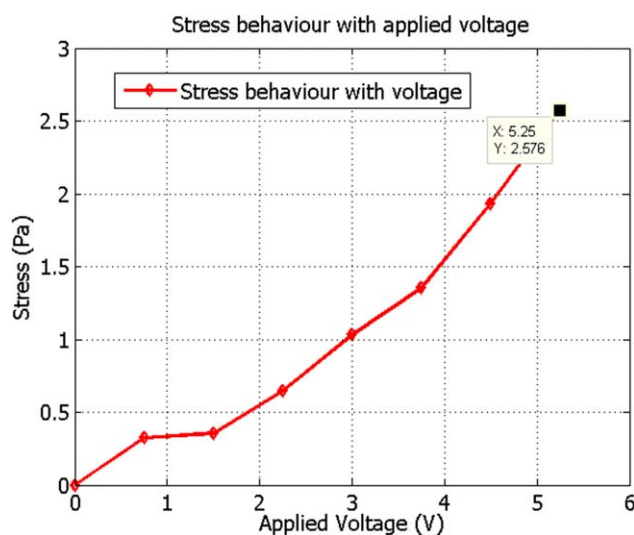


Figure 9. Stress behavior of the SPVA-PANI-Pt ionic membrane. [Color figure can be viewed in the online issue, which is available at wileyonlinelibrary.com.]

To measure the force behavior of the SPVA-PANI-Pt based ionic actuator, the low-force measuring load cell (model Citizen CX-220, India) was used to measure the load, which ranged from 0.0001 to 220 g, as reported by Inamuddin *et al.*²⁶ The voltage was also measured with a multimeter while an ionic strip was in operation. The obtained experimental values are listed in Table I. To calculate the standard deviation, five different force values (1–5) corresponding to the voltage range 0–5.25 V were taken. With a camera, several experiments were conducted, and the video was processed through an image processing method. The standard deviation was obtained as 0.0262, and the normal distribution for the SPVA-PANI-Pt based ionic actuator was 5.8006; this showed that the repeatability of this actuator was 94.19%. To determine the mechanical properties, the stress behavior after the application of the voltage was envisaged, as shown in Figure 9. We found that the maximum stress of this actuator (2.57 Pa) was generated during the application of voltage.

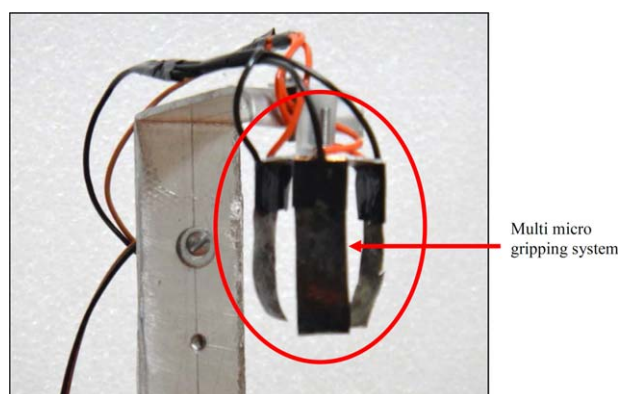


Figure 10. Actual multifinger-based microgripping system with the SPVA-PANI-Pt ionic actuator of the SPVA-PANI-Pt based IPMC actuator. [Color figure can be viewed in the online issue, which is available at wileyonlinelibrary.com.]

After the characterization of the SPVA–PANI–Pt based ionic actuator, a compliant multigripping system along with a control system with SPVA–PANI–Pt based ionic actuator was developed, as shown in Figure 10. The mimicking of fingers was done through electrical actuation instead of a conventional motor. Each finger was actuated individually so that dexterous handling was possible; this allowed precise end-effector positioning. Through the development of this multimicrogripping system, the handling capability with the SPVA–PANI–Pt based ionic actuator was demonstrated. This kind of actuator has potential for handling numerous micrometer- and millimeter-scale components, which can be used in complex fabrication and assembly in robotics.

CONCLUSIONS

In this article, the development of a novel SPVA–PANI–Pt based IPMC actuator by an electroless plating method is reported. The low water loss (48% at 6 V) at an elevated temperature and high water-holding capacity are major advantageous features of this SPVA–PANI–Pt based IPMC actuator. Furthermore, the electromechanical characteristics showed a linear relationship between the deflection and voltage up to 1.8 V. The load-carrying capacity of the actuator was 0.08 gf. With the SPVA–PANI–Pt based IPMC actuator, a compliant multimicrogripping was developed. This has future micro-robotic applications.

ACKNOWLEDGMENTS

The authors are thankful to the Department of Applied Chemistry of Aligarh Muslim University (Aligarh, India) for providing research facilities and to the Department of Science and Technology for giving the Young Scientist Award to Inamuddin (project SR/FT/CS-159/2011). The authors are also thankful to the Central Mechanical Engineering Research Institute (Council of Scientific and Industrial Research, Durgapur, India) for carrying out the electromechanical characterization and for demonstrating the IPMC-based microrobotic system at the DMS/Micro Robotics Laboratory.

REFERENCES

1. Bar-Cohen, Y.; Xue, Y.; Shahinpoor, M.; Salehpoor, V.; Simpson, V.; Smith, V. *Smart Mater. Struct.* **1998**, *3324*, 218.
2. Uchida, M. M.; Taya, M. *Polymer* **2001**, *42*, 9281.
3. Shahinpoor, M.; Bar-Cohen, Y.; Simpson, J. O. *Smart Mater. Struct.* **1998**, *7*, 15.
4. Shahinpoor, M.; Kim, K. J. *Smart Mater. Struct.* **2001**, *10*, 819.
5. Kim, B.; Kim, D. H.; Jung, J.; Park, J. O. *Smart Mater. Struct.* **2005**, *14*, 1.
6. Fang, B. K.; Lin, C. C. K.; Ju, M. S. *Sens. Actuators A* **2010**, *158*, 1.
7. Kim, K. J.; Shahinpoor, M. *Smart Mater. Struct.* **2003**, *12*, 65.
8. Shahinpoor, M.; Kim, K. J. *Smart Mater. Struct.* **2005**, *14*, 197.
9. Han, M. J.; Park, J. H.; Lee, J. Y.; Jho, J. Y. *Macromol. Rapid Commun.* **2006**, *27*, 219.
10. Jeon, J. H.; Kang, S. P.; Lee, S.; Oh, I. K. *Sens. Actuators B* **2009**, *143*, 357.
11. Feng, G. H.; Tsai, J. W. *Smart Mater. Struct.* **2011**, *20*, 015.
12. Fang, Y.; Tan, X. *Sens. Actuators A* **2010**, *158*, 121.
13. Nasser, S. N. *J. Appl. Phys.* **2002**, *92*, 2899.
14. Nasser, S. N.; Wu, Y. *J. Appl. Phys.* **2003**, *93*, 5255.
15. Panwar, V.; Lee, C.; Ko, S. Y.; Park, J. O.; Park, S. *Mater. Chem. Phys.* **2012**, *135*, 928.
16. Panwar, V.; Cha, K.; Park, J. O.; Park, S. *Sens. Actuators B* **2012**, *161*, 460.
17. Holmberg, S.; Holmlund, P.; Nicolas, R.; Wilen, C. E.; Kallio, T.; Sundholm, G.; Sundholm, F. *Macromolecules* **2004**, *37*, 9909.
18. Nguyen, V. K.; Yoo, Y. *Sens. Actuators B* **2007**, *123*, 183.
19. Akle, B. J.; Leo, D. J.; Hickner, M. A.; McGrath, J. E. *J. Mater. Sci.* **2005**, *40*, 3715.
20. Inamuddin; Khan, A.; Luqman, M.; Dutta, A. *Sens. Actuators A* **2014**, *216*, 295.
21. Wang, F.; Chen, T. L.; Xu, J. P. *Macromol. Chem. Phys.* **1998**, *199*, 1421.
22. Wang, X. L.; Oh, I. K.; Lu, J. *Mater. Lett.* **2007**, *61*, 5117.
23. Bai, Z.; Durstock, M. F.; Dang, T. D. *J. Membr. Sci.* **2006**, *281*, 508.
24. Wang, X. L.; Oh, I. K.; Cheng, T. H. *Polym. Int.* **2010**, *59*, 305.
25. Khan, A.; Inamuddin, Jain, R. K.; Naushad, M. *RSC Adv.* **2015**, *5*, 91564.
26. Inamuddin; Khan, A.; Jain, R. K.; Naushad, M. *Smart Mater. Struct.* **2015**, *24*, 095003.
27. Inamuddin; Khan, A.; Jain, R. K.; Naushad, M. *J. Intell. Mater. Syst. Struct.*, to appear.
28. Inamuddin; Jain, R. K.; Hussain, S.; Naushad, M. *RSC Adv.* **2015**, *5*, 84526.
29. Luqman, M.; Lee, J. W.; Moon, K. K.; Yoo, Y. T. *J. Ind. Eng. Chem.* **2011**, *17*, 49.
30. Vargantwar, P. H.; Shankar, R.; Krishnan, A. G.; Ghosh, T. K.; Spontak, R. J. *Soft Matter* **2011**, *7*, 1651.
31. Kim, O.; Shin, T. J.; Park, M. J. *Nat. Commun.* **2013**, *4*, 2208.
32. Rajagopalan, M.; Oh, I. K. *ACS Nano* **2011**, *5*, 2248.
33. Vilen, B.; Marcoux, P. R.; Lekka, M.; Sienkiewicz, A.; Feher, T.; Forro, L. *Adv. Funct. Mater.* **2006**, *16*, 120.
34. Li, J.; Vadahanambi, S.; Kee, C. D.; Oh, I. K. *Biomacromolecules* **2011**, *12*, 2048.
35. Panwar, V.; Kang, B. S.; Park, J. O.; Park, S. H. *Eng. Sci.* **2011**, *51*, 1730.
36. Nguyen, V. K.; Lee, J. W.; Yoo, Y. T. *Sens. Actuators B* **2007**, *120*, 529.
37. Kariduraganavar, M. Y.; Kulkarni, S. S.; Kittur, A. A. *J. Membr. Sci.* **2005**, *246*, 83.
38. Fan, H.; Wang, H.; Zhao, N.; Zhang, X.; Xu, J. *J. Mater. Chem.* **2012**, *22*, 2774.